Physics in Medicine & Biology

IPEM
Institute of Physics and Engineering in Medicine

PAPER

Realization of fluence field modulated CT on a clinical TomoTherapy megavoltage CT system

To cite this article: Timothy P Szczykutowicz *et al* 2015 *Phys. Med. Biol.* **60** 7245

View the article online for updates and enhancements.

You may also like

- TMS intensity and focality correlation with coil orientation at three non-motor regions
Jose Gomez-Feria, Mariano Fernandez-Corazza, Juan F Martin-Rodriguez et al.
- Inclusion of quasi-vertex views in a brain-dedicated multi-pinhole SPECT system for improved imaging performance
Benjamin Auer, Navid Zeraatkar, Justin C Goding et al.
- Practical joint reconstruction of activity and attenuation with autonomous scaling for time-of-flight PET
Yusheng Li, Samuel Matej and Joel S Karp

SunCHECK®
Powering Quality Management in Radiation Therapy
See why 1,600+ users have chosen SunCHECK for automated, integrated Patient QA and Machine QA.
Learn more >

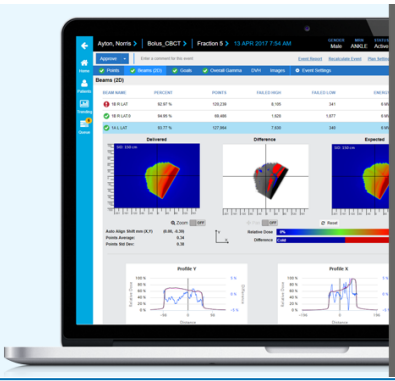

Demo SunCHECK at ESTRO:
Booth # 150
SUN NUCLEAR

This content was downloaded from IP address 128.179.149.227 on 21/06/2023 at 16:17

IOP Publishing | Institute of Physics and Engineering in Medicine Physics in Medicine & Biology

Phys. Med. Biol. **60** (2015) 7245–7257 doi:10.1088/0031-9155/60/18/7245

Realization of fluence field modulated CT on a clinical TomoTherapy megavoltage CT system

Timothy P Szczykutowicz[1,2,3], James Hermus[3], Mark Geurts[4] and Jennifer Smilowitz[2,4]

[1] Department of Radiology, University of Wisconsin-Madison, Madison WI 53705, USA
[2] Department of Medical Physics, University of Wisconsin-Madison, Madison WI 53705, USA
[3] Department of Biomedical Engineering, University of Wisconsin-Madison, WI 53706, USA
[4] Department of Human Oncology, University of Wisconsin-Madison, WI 53705, USA

E-mail: tszczykutowicz@uwhealth.org

Received 4 February 2015, revised 8 July 2015
Accepted for publication 29 July 2015
Published 7 September 2015

Abstract

The multi-leaf collimator (MLC) assembly present on TomoTherapy (Accuray, Madison WI) radiation therapy (RT) and mega voltage CT machines is well suited to perform fluence field modulated CT (FFMCT). In addition, there is a demand in the RT environment for FFMCT imaging techniques, specifically volume of interest (VOI) imaging.

A clinical TomoTherapy machine was programmed to perform VOI. Four different size ROIs were placed at varying distances from isocenter. Projections intersecting the VOI received 'full dose' while those not intersecting the VOI received 30% of the dose (i.e. the incident fluence for non VOI projections was 30% of the incident fluence for projections intersecting the VOI). Additional scans without fluence field modulation were acquired at 'full' and 30% dose. The noise (pixel standard deviation) and mean CT number were measured inside the VOI region and compared between the three scans. Dose maps were generated using a dedicated TomoTherapy treatment planning dose calculator.

The VOI-FFMCT technique produced an image noise 1.05, 1.00, 1.03, and 1.05 times higher than the 'full dose' scan for ROI sizes of 10 cm, 13 cm, 10 cm, and 6 cm respectively within the VOI region. The VOI-FFMCT technique required a total imaging dose equal to 0.61, 0.69, 0.60, and 0.50 times the 'full dose' acquisition dose for ROI sizes of 10 cm, 13 cm, 10 cm, and 6 cm respectively within the VOI region.

 © 2015 Institute of Physics and Engineering in Medicine Printed in the UK

Noise levels can be almost unchanged within clinically relevant VOIs sizes for RT applications while the integral imaging dose to the patient can be decreased, and/or the image quality in RT can be dramatically increased with no change in dose relative to non-FFMCT RT imaging. The ability to shift dose away from regions unimportant for clinical evaluation in order to improve image quality or reduce imaging dose has been demonstrated. This paper demonstrates that FFMCT can be performed using the MLC on a clinical TomoTherapy machine for the first time.

Keywords: CT, FFMCT, dynamic bowtie, volume of interest imaging, IGRT

(Some figures may appear in colour only in the online journal)

1. Introduction

As radiation therapy (RT) dose delivery systems have progressed, they have allowed for better healthy tissue sparing due to their ability to deliver higher dose gradients. In order to take advantage of high dose gradients, however, the location of the tumor and healthy tissue must be confirmed prior to treatment. TomoTherapy (Accuray, Madison WI) is a commercially available RT system that combines pretreatment imaging with intensity modulated delivery (IGRT) (Mackie 2006, Shah *et al* 2008). Prior to an IGRT treatment, the patient is given a computed tomography (CT) scan to verify target location and adjust patient position if needed. This is ensured by registering the borders of the patient's tumor to the treatment region. In addition, the radiation oncologist can monitor any gross changes in the patient's morphology due to weight loss/gain, or changes in body positioning.

The focus of this paper is on the imaging involved in IGRT; we propose that since radiation oncologists only need good image quality for a small volume of interest (VOI) within a patient's cross section, we should only create a high quality image within that VOI. VOI imaging provides a method for (1) keeping the total imaging dose the same relative to unmodulated imaging while increasing the image quality inside the VOI, (2) to reduce the imaging dose while maintaining image quality within a VOI, or (3) to increase the image quality within the VOI and reduce the integral imaging dose to the patient. As stated in AAPM Task Group Report Number 75, 'radiographic guidance techniques have one thing in common, they can give a significant radiation dose to the patient' (Murphy *et al* 2007). VOI imaging would allow for the imaging dose inside a VOI region, a region that will likely be receiving a very large treatment dose, to remain unchanged from what is currently delivered while the rest of the patient's body could receive a much lower dose. The total dose could be tuned to whatever clinical need was required. The important point here is that without FFMCT, one is left without the means to regionally prescribe image quality and therefore imaging dose. Typically, the integral image dose is about 1% of the treatment dose (Murphy *et al* 2007, Shah *et al* 2008). With such a large difference in dose, one may wonder why dose reduction in RT is important. While it is true that the treatment dose is much higher the imaging dose, it is also true that the treatment dose is not delivered uniformly within the patient. Outside the treatment volume, it is common for the treatment dose to decrease significantly, often by a factor of 2 or 3 over a few centimeters of tissue (Shah *et al* 2008). Therefore, while not a large fraction of the dose received within a patient's treatment volume, the dose received from imaging contributes a non-trivial portion of the dose outside a patient's treatment volume. The region outside of the treatment volume is usually healthy tissue that ideally would receive no dose during image or treatment.

Poor image quality has plagued RT since IGRT was developed. This is mainly due to the low contrast inherent with TomoTherapy's high beam energy (Ruchala *et al* 1999) and the large scatter fraction present in linac based IGRT (Bootsma *et al* 2011). Therefore, methods for increasing image quality that are dose neutral or reduce dose to healthy tissue should benefit patient care in the RT environment.

Recent advances in the field of CT imaging should aide the radiation oncologist in obtaining higher quality pretreatment images with no radiation dose increase (Bartolac *et al* 2011, Hsieh and Pelc 2013a, Szczykutowicz and Mistretta 2013a, 2013b, Szczykutowicz and Mistretta 2014). This is possible through the application of fluence field modulated computed tomography (FFMCT) technology to the current TomoTherapy MVCT acquisition. FFMCT actually takes a page from the book of intensity modulated radiation therapy (IMRT) by modulating the imaging dose incident onto the patient as a function of rotation angle. Through the use of FFMCT applied to TomoTherapy CT (FFMCT-MVCT) acquisitions, it should be possible to increase the image quality within a pre-determined volume of interest while decreasing the image quality outside the VOI (Kolditz *et al* 2010, Chen *et al* 2011, Heuscher and Noo 2011, 2012, Oktay and Noo 2014, Szczykutowicz and Hermus 2015). The integral imaging dose can be adjusted to remain the same as for a non-FFMCT-MVCT acquisition. Thus, with FFMCT-MVCT, the radiation oncologist could get better image quality where they need it at no cost in radiation dose to the patient. Even if the dose is raised to levels considered excessive in diagnostic CT, this dose can be incorporated into the patient's RT treatment plan, effectively mitigating imaging dose concerns for the patient.

FFMCT on a TomoTherapy system is straight forward as TomoTherapy systems already have the necessary hardware to enable FFMCT imaging. The multi-leaf collimator (MLC) used for intensity modulated RT (see figure 1) can also be used for FFMCT as will be first demonstrated in this paper. Some early TomoTherapy work did consider using projection data acquired during treatment to reconstruct CT images, but obtaining artifact free images was hindered by many technical issues as shown by Ruchala *et al* (2000). Use of FFMCT in the radiation therapy clinic would also be possible on linac based radiation therapy systems with on-board flat panel imaging systems using a dynamic collimator (Hsieh and Pelc 2013a, Szczykutowicz and Mistretta 2014) or possibly using a MLC designed for RT. The results shown in this paper were generated with no hardware or software changes to our clinical TomoTherapy system; this suggests that this application of FFMCT technology can be easily adopted in the clinic. To better understand how a MLC can be used for FFMCT, we have also shown a depiction of the location of the bowtie filter used in diagnostic CT and an image of an actual bowtie filter in figure 1.

2. Methods

2.1. System geometry

TomoTherapy radiation therapy machines use a 3.5 MV photon beam to image patients. The geometrical specifications for TomoTherapy machines are: source to detector distance = 132.3 cm, source to iso-center distance = 85 cm, source to MLC = 20 cm, number of MLC leaves = 64, number of detectors elements equal to 640, number of detector rows = 1, and a fan angle of 26.8°. The multi-leaf collimator assembly is designed to totally attenuate the 6 MV treatment beam. During treatment, the number of therapy photons incident on the patient is modulated by varying the so called 'leaf open time'. In other words, for each treatment angle, the linac produces 6 MV treatment photons (usually at a frequency of ≈300 Hz) and the amount of radiation incident on the patient is controlled by how long the collimator leaf blocks

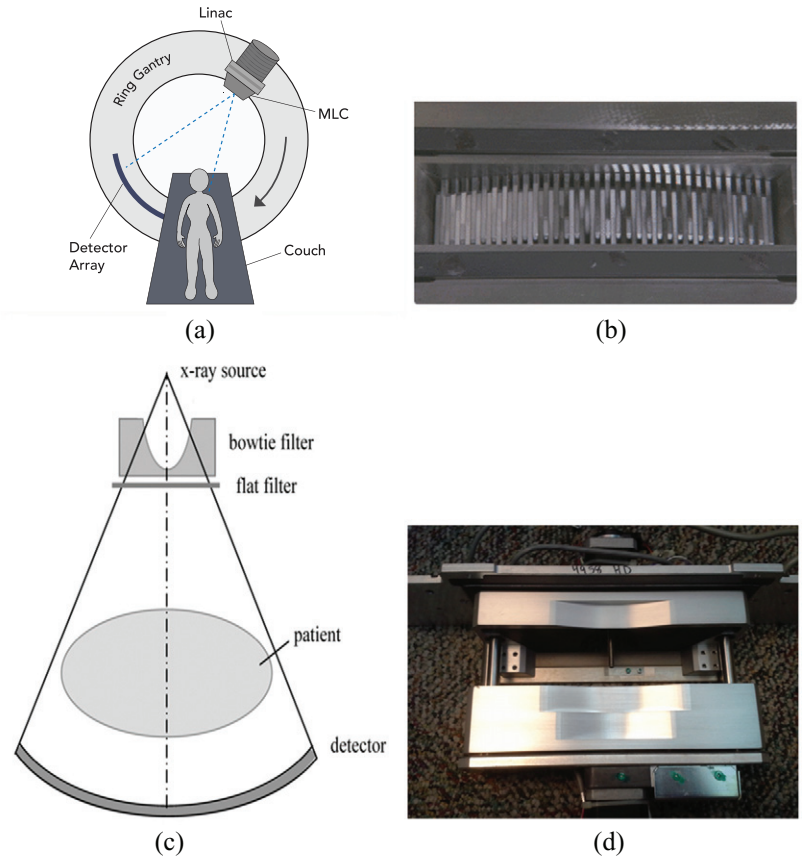

Figure 1. (a) Schematic of a TomoTherapy system, including the location of the MLC. Note how the MLC is positioned much like a bowtie filter in diagnostic CT. (b) A picture of the MLC present on a TomoTherapy system, the 64 individual collimator leaves can be seen. (c) Depiction of where a bowtie filter is positioned within a diagnostic CT scanner. (d) Image of a bowtie filter from a modern diagnostic CT scanner. This particular bowtie filter has three different size filter filters on a single assembly. These filters cannot be changed during a scan to allow for view angle modulation of the fluence profile. (c) Reproduced with permission from Hsieh (2003).

the beam. To implement FFMCT, the MLC can be used to modulate the number of imaging photons incident onto a patient as a function of view angle. This approach actually has a key advantage over the attenuation based modulation proposed by Hsieh and Pelc (2013a) and Szczykutowicz and Mistretta (2013a, 2013b, 2014) in that the mean beam energy change due to hardening of the beam by the filtering material is not present in this application. When a leaf is closed on a TomoTherapy system, the field is completely attenuated.

2.2. Data aqusition

Raw projection data was obtained from a clinical TomoTherapy unit at our institution. The TomoTherapy imaging and treatment beam is pulsed; each pulse can be recorded by the TomoTherapy CT detector. We acquired projection data sets using a tissue characterization phantom (Gammex Number 467, Middelton, WI). The phantom is 33 cm in diameter and

5 cm thick. We acquired a total of 6 CT acquisitions of this phantom. For all scans, we set the linac pulse rate to 80 Hz, the gantry rotation time to 60 s, the table speed to 0 mm s^{-1}(axial mode), and we acquired 180 view angles over 360 degrees. The leaflet sinogram for the 'full dose' scan had all leaves open 100% of the time for each view angle. For the 30% dose scan, we used the same acquisition parameters except the leaves were programmed to only open for 30% of the time required for each view angle. For a pulse rate of 80 Hz, 180 view angles, and a 360 view angular range, on average 26.7 pulses formed a single view angle. Therefore, in order to modulate the image dose down to 30%, the leaves were programmed to only let through 8 pulses. Four different sized VOI were imaged at four different distances from iso-center as shown in figure 3. A 10 cm diameter VOI was located centered on iso-center, a 13 cm diameter VOI was located 2 cm from iso-center at the 9 o'clock position, a 10 cm diameter VOI was located 5 cm from iso-center at the 12 o'clock position, and a 6 cm diameter VOI was located 6 cm from iso-center at the 3 o'clock position. For each VOI acquisition, all collimator leaves that intersected the VOI were set to have leaf open times of 100%. All leaves not intersecting the VOI were set to only open for 30% of the time for each view angle. An example of TomoTherapy projection data is shown in figure 2. The difference between a non-FFMCT and a FFMCT data acquisition is easy to observe as within each view angle the FFMCT scan acquires less pulses relative to the non-FFMCT scan.

All images were reconstructed using an FBP algorithm (Kak 1979) with a ramp reconstruction kernel. The image reconstruction field of view was 350 mm for all images using a pixel dimension of 512 by 512.

Scans were acquired both with the phantom in place, and with the phantom and couch removed from the bore (i.e. air scan). This allowed for CT projections to be obtained by log normalizing the phantom data with 'air scan' data. Image quality comparisons were made by comparing the noise level (standard deviation in voxel values from within a uniform region) and mean reconstructed image value in ROI's placed inside the VOI. The ROI locations are shown in figure 3. Difference images were also generated to qualitatively understand if certain regions of the VOI images were more accurate than others relative to the 'full dose' acquisition.

2.3. Dose calculation

Dose was calculated using a software package and workstation provided by Accuray. The dose calculator was the same as used by Shah *et al* (2008). A kilovoltage CT scan acquired using a diagnostic CT scanner was taken of the phantom following our RT clinic's usual work flow. This image was used to obtain the physical density image required for the dose calculation.

Relative dose maps were generated in which the absolute dose image for the 'full dose' case was used to normalize the dose for each of the other cases. In addition, the total dose the phantom received in the central plane of the phantom was summed for each case. This sum was only taken over the phantom by excluding the dose to air and the couch. The total dose to the phantom was reported relative to the 'full dose' and 30% dose cases.

3. Results and discussion

Six images were reconstructed as shown in figure 4. By comparing a 'full dose', 30% dose, and the four VOI-FFMCT images, it is easy to observe how the VOI-FFMCT scan allows for image quality equal to the 'full dose' scan within the VOI while providing image quality

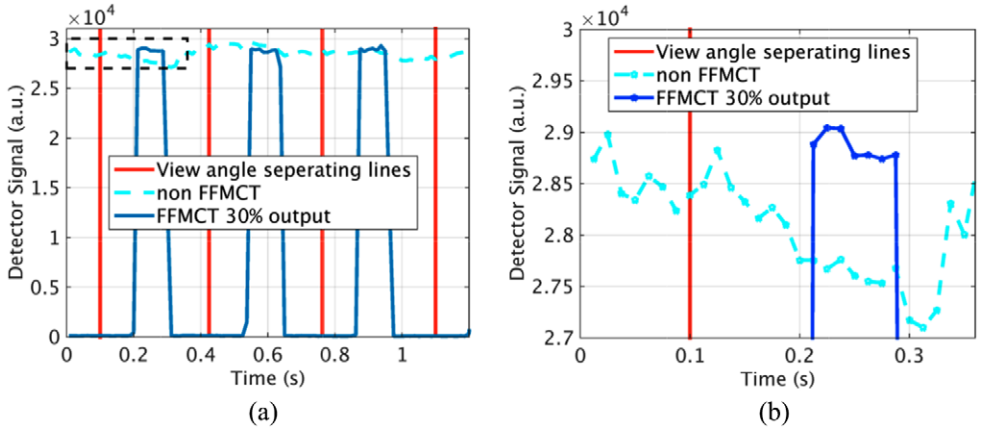

Figure 2. Plot of raw TomoTherapy data. The data has not yet been binned into view angles and each linac pulse can be observed. The pulse frequency was 80 Hz for the data shown in these plots. Depicted in (a) is both a non FFMCT scan and a detector row corresponding to the 30% modulated region of a FFMCT scan. Depicted in (b) is a zoomed in version of (a) to allow for better visualization of the difference between a non-FFMCT and a FFMCT scan and to better understand the implementation of FFMCT using discrete pulses of radiation.

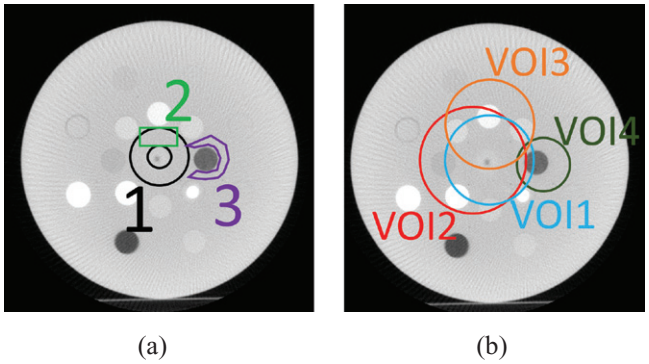

Figure 3. (a) Depiction of the ROI locations used to measure the noise values reported in table 1. The voxels defined by ROI 1 (black ROI centered at isocenter) were used to measure the noise for the images shown in figures 4(a)–(d) (The 'full dose', 30% dose, VOI1 and VOI2 used ROI 1). The voxels defined by ROIs 2 (green rectangular ROI at 12 o'clock) and 3 (purple ROI at 3 o'clock) were used to measure the noise for the images shown in figure 4(e) (VOI3) and figure 4(f) (VOI4), respectively. Noise and mean ROI values are reported in table 1. (b) Location of the VOIs.

closer to the 'low dose' image outside the VOI. The noise (voxel standard deviation), measured inside the VOI for each image over a uniform region are reported in table 1.

Obvious in figure 4 are the under-sampling artifacts in the VOI-FFMCT outside of the VOI. The undersampling artifacts are due to the use of only 180 view angles. Based on the system geometry specifications given in section 2.1, 1,724 views angles would be required to ensure aliasing free sampling (Natterer 1993). Albeit typical diagnostic CT scanners rarely follow this sampling requirement. Clinical TomoTherapy patient confirmation scans are acquired with around 800 view angles. The scans performed in the present work were limited to 180

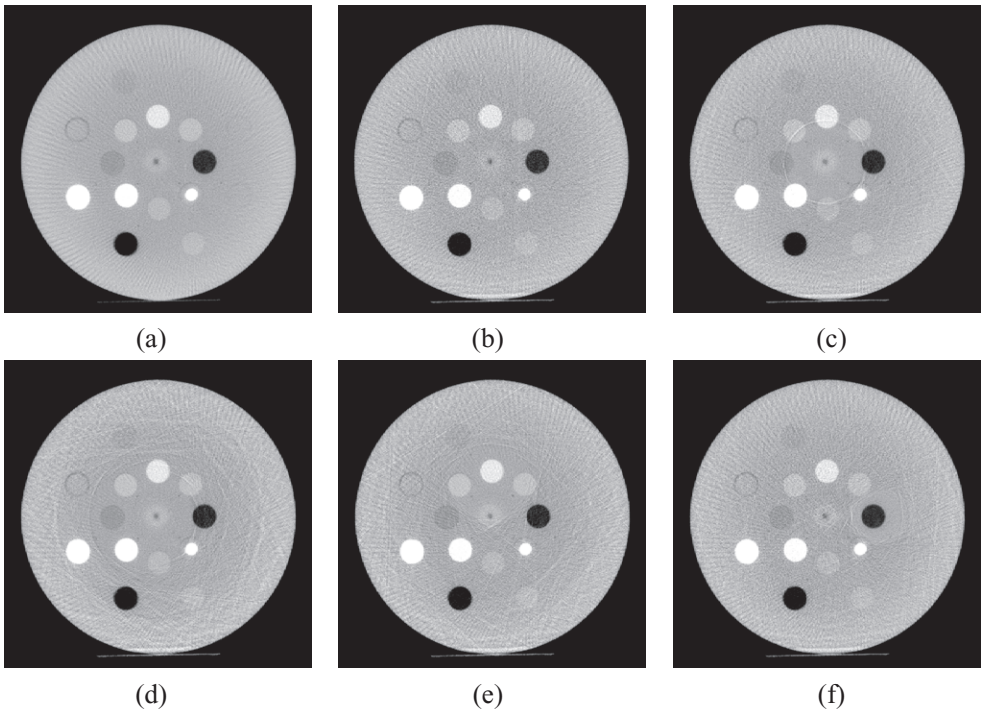

Figure 4. Using a clinical TomoTherapy machine, a 'full dose' MVCT image (a), and a 30% dose MVCT image (b) were acquired. Additionally, 4 different size VOI images were acquired at varying distances from iso-center. (c) A 10 cm diameter VOI located on iso-center, (d) a 13 cm diameter VOI located 2 cm from iso-center, (e) a 10 cm diameter VOI located 5 cm from iso-center, and (f) a 6 cm diameter VOI located 6 cm from iso-center. All images displayed at [0.031 0.093] cm^{-1}. (a) ('full dose'). (b) (30% dose). (c) (VOI1). (d) (VOI2). (e) (VOI3). (f) (VOI4).

Table 1. Image noise and mean ROI value comparison.

Acquisition	Noise[a] (cm^{-1})	Noise relative to 'full dose'	Noise relative to 30% dose	Mean ROI value (cm^{-1})
'full dose'	0.00022	1.00	0.50	0.0072
30% dose	0.00045	2.00	1.00	0.0072
VOI1	0.00023	1.05	0.53	0.0073
VOI2	0.00022	1.00	0.50	0.0072
VOI3	0.00023	1.03	0.52	0.0073
VOI4	0.00024	1.05	0.53	0.0073

[a]The noise values are standard deviations measured from uniform ROIs as shown in figure 3.
Note: VOI1-4 refer to the images shown in figures 4(c) and (d) respectively.

view angles to increase the granularity of dose modulation. The number of pulses per view angle (N_p) is given by the pulse rate (P) times the rotation time (T) divided by the number of view angles (N_v),

$$N_p = \frac{PT}{N_v}. \quad (1)$$

As the number of view angles increases, the number of pulses per view angle decreases. In this study, on average, 27 pulses were used for each view angle. A 30% modulation only used 8 of these pulses. If the number of view angles were increased to 1,000, only 4.8 pulses on average would be used for each view angle. Such a low number of pulses limits the ability to have a high level of granularity in modulation level. For example, with 1,000 view angles, only ≈0%, 20%, 40%, 60%, 80%, and 100% modulation levels would be possible corresponding to using 1, 2, 3, 4, or 5, pulses. The current experiments were performed using 80 Hz for the pulse rate. The TomoTherapy platform is capable of using 300 Hz which should allow for higher numbers of view angles in addition to a higher degree of modulation level granularity.

Some of the images in figure 4 exhibit artifact in the regions outside the VOI. The artifact takes the form of a streaking artifact and does not form rings as the occurrence is not constant as a function of view angle for the same detector position. These artifacts are most easily observed in figures 4(d) and (e). The root cause of these artifacts is under investigation but is believed to be dependent on the number of leaves that are requested to move within a given time period. As the number of leaves requested to move at the same time increases, the degree of artifact gets worse. This is evident by noting the worst artifact level is present in the VOI scan with the largest VOI. If the number of pulses is unequal between the phantom and air-scan, these artifacts are present. This was confirmed by analyzing the air scan and phantom projection data. In addition to being unequal in pulse number, it is also possible for pulses to be 'clipped' by a collimator leaf before the pulse is recorded by the detector. This results in only part of the pulse getting recorded by the detector. These artifacts should not be an issue for the intended purpose of VOI-FFMCT images in the radiation therapy setting. The image quality outside of the VOI can be quite limited. For daily setup, physicians often only need to identify gross changes in patient positioning and therefore need to be able to observe the external contour (i.e. skin line), bony anatomy landmarks, and tissue-air interfaces (e.g. lung, stomach, intestines). All of the images shown in figure 4 would allow for this.

The difference in noise inside the VOIs relative to the 'full dose' case was less than 5% for all VOI cases. The dependence of this difference in noise to VOI size and position from iso-center will be the focus of a future work. Intuitively, as the VOI size becomes larger it would be expected the image quality inside the VOI should approach that of the 'full dose' case.

Figure 5 shows the difference images for each VOI case with respect to the 'full dose' case. The mean signal level within the VOI region is slightly higher in some of the VOI scans relative to the 'full dose' case. This is also apparent in table 1. These differences, however, are all within 1% of the 'full dose' case. The 30% dose non-modulated scan does show mis-registration artifacts as it was acquired several minutes after the 'full dose' image and the phantom shifted slightly during that time. The structure most easily observed in the difference images, excluding the mis-registration artifacts, is the small high density 'bone like' insert positioned at the 5 o'clock position. This structure can be observed on all of the VOI scans. The difference between this structure and the 'full dose' image, however, is equal to the difference between the mean difference within the VOIs which is 1%. For the intended purposes of this VOI-FFMCT radiotherapy application, this difference is negligible.

3.1. Relative dose comparisons

As expected, the dose delivered for each VOI case was less than the 'full dose' case and larger than the 30% dose case. These results are listed in table 2. The dose scaled with the VOI size as can be observed in table 2. The largest VOI required a dose of 0.69 times the 'full dose' case while the smallest VOI required half the dose of the 'full dose' case. The relative dose maps

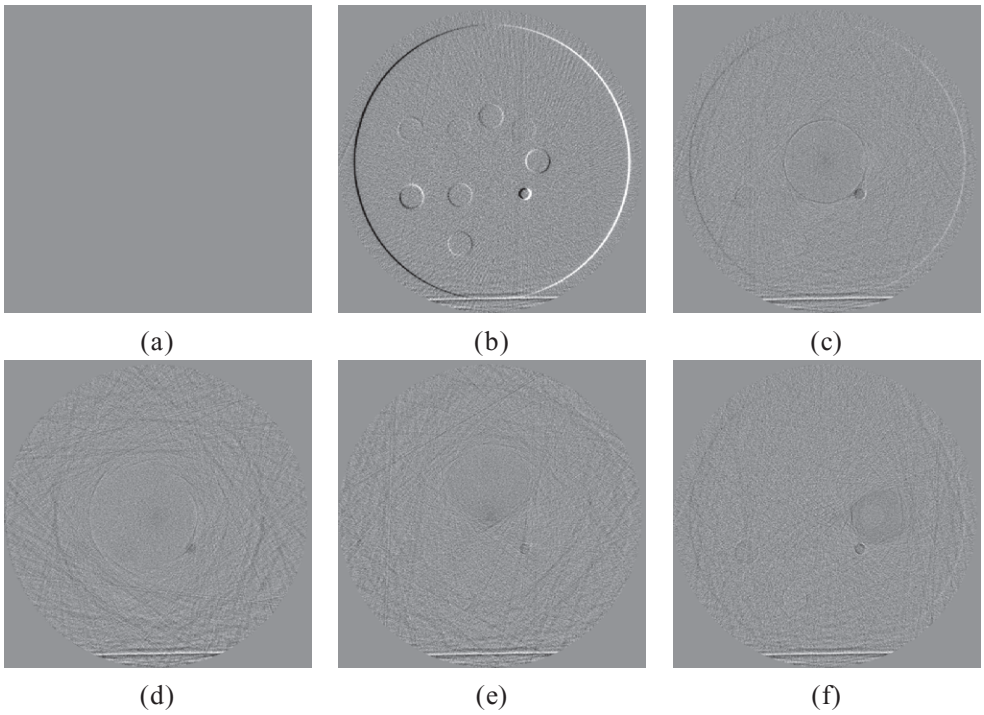

Figure 5. Difference between each image in figure 4 with the 'full dose' case. (a) 'full dose' case, (b) 30% dose case, (c) the 10 cm diameter VOI located on iso-center difference, (d) the 13 cm diameter VOI located 2 cm from iso-center difference, (e) the 10 cm diameter VOI located 5 cm from iso-center difference, and (f) the 6 cm diameter VOI located 6 cm from iso-center difference. All images displayed at [−0.0005 0.0005] cm^{-1}. Figures 4(a), (c)–(f) were acquired sequentially in time. There was a few minutes delay before the acquisition of image 4(b) during which time the phantom shifted, causing the slight mis-registration artifacts in (b). All images displayed at [−0.0025 0.0025] cm^{-1}.

shown in figure 6 show that most of the phantom outside the VOI regions had dose levels at or smaller than half of the 'full dose' case. The dose inside the VOI region is about 0.9 times that of the 'full dose' case. This percentage increases slightly as the VOI size increases. One would expect the VOI dose to be slightly less than the 'full dose' case due to scatter. While it is true the VOI will receive the same number of primary photons as the 'full' dose case, the amount of scatter radiation contributing to the dose inside the VOI will be smaller for the VOI cases relative to the 'full dose' case. This is because less primary radiation is incident onto the patient for rays outside the VOI which results in less scatter being produced outside the VOI capable of depositing dose inside the VOI. A reduction in scatter has been shown previously in the field of FFMCT in diagnostic imaging with some cases showing reductions in scatter-to-primary ratio of as large as 4 times (Szczykutowicz and Mistretta 2013b). These results, however, are not directly comparable to the present work because the beam energy used in TomoTherapy is in the mega-voltage range compared to the kilo-voltage range of diagnostic imaging. More work remains to be done in quantifying the scatter reductions possible with FFMCT at all beam energies and for all applications of FFMCT including optimized bowtie filtering and VOI applications.

Table 2. Relative integral dose comparisons between the VOI modes.

Acquisition	Dose relative to 'full dose'	Dose relative to 30% dose	VOI diameter (cm)	VOI distance from isocenter[a] (cm)
'full dose'	1	3.33	n/a	n/a
30% dose	0.3	1	n/a	n/a
VOI1	0.61	2.0	10	0
VOI2	0.69	2.3	13	2
VOI3	0.6	2.0	10	5
VOI4	0.5	1.7	6	6

[a]The distance from isocenter to the center of the VOI.
Note: Dose was summed from the center slice of the phantom and normalized by the 'full dose' case.

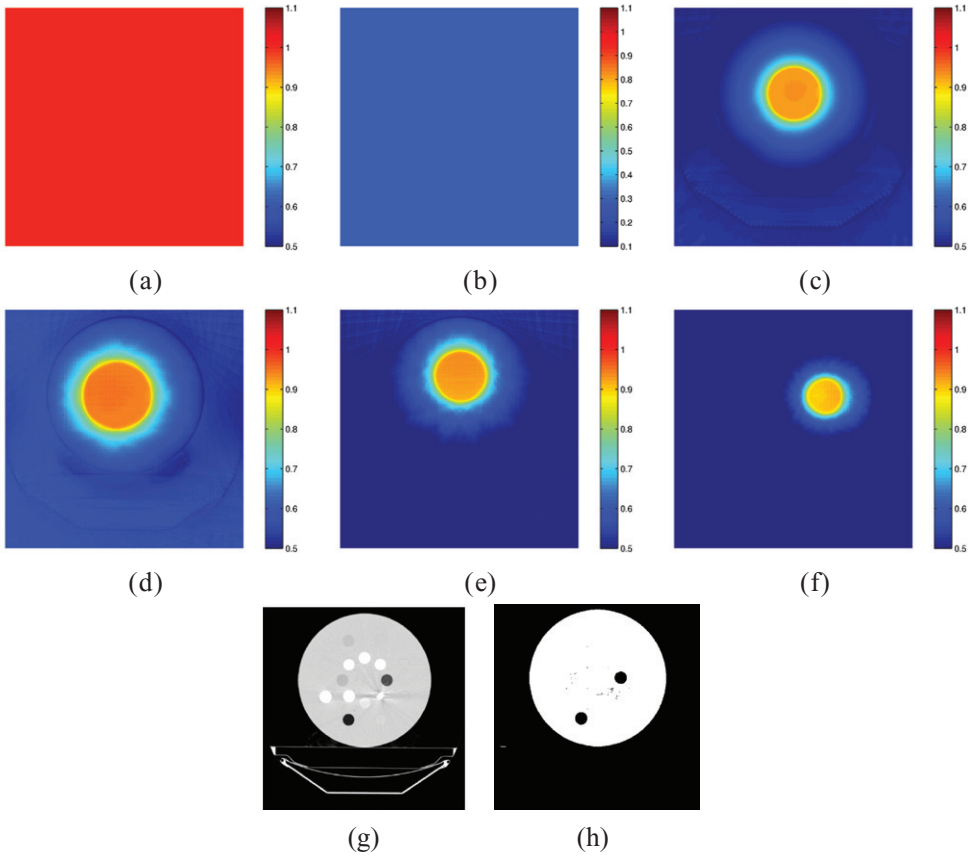

Figure 6. (a)–(f) Relative dose maps for each of the acquisition modes shown in figure 4, respecively. All doses are relative to the 'full dose' case. (g) Is an image of the CT image used for the dose calculations and (h) is the mask applied to the dose distributions that allows for air and the couch to be excluded from the dose comparisons.

Based on these results, the possible benefit of FFMCT applied to MVCT in the RT IGRT workflow can be seen. For a given IGRT registering task, image quality could be held constant inside a sub region of clinical interest while the total imaging dose is reduced. In our results, if the clinically relevant region was 6 cm in diameter, the total dose could be cut in half

without sacrificing image quality inside the VOI. Additionally, it would be possible to increase the image quality within the VOI region while keeping the total imaging dose constant. A third option would also be possible. One could simultaneously achieve a dose reduction and increase the image quality inside some pre-defined region.

4. Conclusions

Based on qualitative image analysis of our FFMCT images and the difference between FFMCT and 'full dose' non-FFMCT images, the image quality achievable inside the VOIs is equal to that of the 'full dose' non-FFMCT images. Noise standard deviation and mean signal measurements confirmed this. Future work will aim to re-produce our results using a more realistic CT acquisition in which the gantry rotation time is lowered to the 6–10 s range and the acquisition and reconstruction are helical instead of axial.

We will also further characterize the source of the artifacts outside of the VOI regions. Even though these artifacts should be easily tolerated for the imaging tasks present outside the VOI, mitigating these artifacts is still a priority. As mentioned in section 3, the two causes of artifacts outside of the VOI region are believed to be caused by a mis-match between the number of pulses and by pulses getting clipped to varying degrees between the air-scan and the patient scan. Currently, our group is working on an algorithm to detect when a given pulse is clipped and to measure the number of pulses used per projection. When a projection is determined to contain a clipped pulse or the pulse number changes between the air and patient scans, we have successfully been able to remove these pulses from both the air-scan and patient scan data sets and reconstruct images with no artifacts. This is still a work in progress.

As mentioned in the introduction, this work should allow for a dose reduction of healthy tissue outside of the treatment volume. While the total imaging dose is small compared to the treatment dose in most cases, it should not be considered trivial (Murphy *et al* 2007, Olch *et al* 2007, Shah *et al* 2008) especially for pediatric cases where fear of treatment/imaging induced cancers is a concern. Future work will include applying FFMCT imaging methods to clinical CT datasets and calculating the anticipated changes in dose as a function of VOI size, shape, and location.

This work applies FFMCT technology to a RT clinic treatment delivery system for the first time. The use of FFMCT in the RT setting will enable radiation oncologists to define regions of high and low image quality much like they do with dose. These regions could be defined in an automated manner simply by assuming an extra margin needs to be added to the treatment border. Since the structure set is stored as part of the Radiation Therapy DICOM standard format, the location of the treatment regions with respect to the imaging geometry of the TomoTherapy system can be determined. Our group has performed proof-of-concept studies in which treatment locations were extracted from DICOM planning images, an optional extra margin was added to account for patient set-up errors, and FFMCT TomoTherapy sinograms were created by forward projection as described in this paper. This workflow does not require any additional contouring and could be automated. Targets could be identified by their structure name, e.g.: PTV50Gy. The free parameters would be the desired margin thickness to add to the treatment region and the desired difference between image quality inside and outside of the treatment region. Other contoured regions could also easily be incorporated into this workflow to either reduce or enhance the image quality/dose to specific structures or regions.

The use of a TomoTherapy system for FFMCT may also be useful for kV CT and CBCT researchers seeking to evaluate FFMCT. Advanced numerical methods for controlling fluence distributions are being developed (Bartolac *et al* 2010, 2011, Bartolac and Jaffray 2012, Hsieh

and Pelc 2013b), but experimental apparatus to test these algorithms on is currently in the development stages by a few groups around the world. TomoTherapy systems enjoy a large distribution and may be a viable alternative to evaluating FFMCT methods. It is promising that no hardware or software changes were required for the scanner to implement FFMCT. This may allow for rapid utilization by the RT community and facilitate FFMCT research on these systems by other groups.

Acknowledgments

We acknowledge Drs R Mackie and J Bayouth for fruitful discussions regarding clinical applicability and technical considerations. Accuray Inc. provided the research workstation used for dose calculation through a collaboration agreement.

References

Bartolac S, Graham S, Siewerdsen J and Jaffray D 2010 Compensator approaches for intensity modulated computed tomography *Int. Conf. on Image Formation in X-ray Computed Tomography* vol 1 p 101

Bartolac S, Graham S, Siewerdsen J and Jaffray D 2011 Fluence field optimization for noise and dose objectives in CT *Med. Phys.* **38** S2–17

Bartolac S and Jaffray D 2012 Fluence field modulated computed tomography *Int. Conf. on Image Formation in X-ray Computed Tomography* vol 2 pp 119–22

Bootsma G, Verhaegen F and Jaffray D 2011 The effects of compensator and imaging geometry on the distribution of x-ray scatter in CBCT *Med. Phys.* **38** 897–914

Chen L, Yu L, Leng S and McCollough C 2011 CT volume-of-interest (VOI) scanning: determination of radiation reduction outside the VOI *Conf. Radiological Society of North America* SSK15-07

Heuscher D and Noo F 2011 CT dose reduction using dynamic collimation *IEEE Nuclear Sci. Symp. and Medical Imaging Conf.* pp 3470–3

Heuscher D and Noo F 2012 CT dose reduction using dynamic collimation *The Second Int. Conf. on Image Formation in X-ray Computed Tomography* pp 115–8

Hsieh J 2003 *Computed Tomography: Principles, Design, Artifacts, and Recent Advances* vol 114 (Bellingham, WA: SPIE Optical Engineering Press)

Hsieh S S and Pelc N J 2013a The feasibility of a piecewise-linear dynamic bowtie filter *Med. Phys.* **40** 031910

Hsieh S S and Pelc N J 2013b Optimized control of a dynamic, prepatient attenuator *SPIE Med. Imaging* **8668** 86681Q

Kak A 1979 Computerized tomography with x-ray, emission, and ultrasound sources *Proc. IEEE* **67** 1245–72

Kolditz D, Kyriakou Y and Kalender W 2010 Volume-of-interest (VOI) imaging in c-arm flat-detector CT for high image quality at reduced dose *Med. Phys.* **37** 2719

Mackie T R 2006 History of tomotherapy *Phys. Med. Biol.* **51** R427

Murphy M J *et al* 2007 The management of imaging dose during image-guided radiotherapy: report of the AAPM task group 75 *Med. Phys.* **34** 4041–63

Natterer F 1993 Sampling in fan beam tomography *SIAM J. Appl. Math.* **53** 358–80

Oktay M and Noo F 2014 Reduction of dose by focusin the x-ray beam to a specific region of interest: Monte Carlo assessment *The Third Int. Conf. on Image Formation in X-ray Computed Tomography* pp 279–82

Olch A J, Geurts M, Thomadsen B, Famiglietti R and Chang E L 2007 Portal imaging practice patterns of childrens oncology group institutions: dosimetric assessment and recommendations for minimizing unnecessary exposure *Int. J. Radiat. Oncol. Biol. Phys.* **67** 594–600

Ruchala K, Olivera G, Kapatoes J, Schloesser E, Reckwerdt P and Mackie T 2000 Megavoltage CT image reconstruction during tomotherapy treatments *Phys. Med. Biol.* **45** 3545

Ruchala K, Olivera G, Schloesser E and Mackie T 1999 Megavoltage CT on a tomotherapy system *Phys. Med. Biol.* **44** 2597

Shah A P, Langen K M, Ruchala K J, Cox A, Kupelian P A and Meeks S L 2008 Patient dose from megavoltage computed tomography imaging *Int. J. Radiat. Oncol. Biol. Phys.* **70** 1579–87

Szczykutowicz T P and Hermus J R 2015 Fluence field modulated CT on a clinical TomoTherapy radiation therapy machine *SPIE Medical Imaging* **9412** 94120U

Szczykutowicz T and Mistretta C 2013a Design of a digital beam attenuation system for computed tomography: Part I. System design and simulation framework *Med. Phys.* **40** 021905

Szczykutowicz T and Mistretta C 2013b Design of a digital beam attenuation system for computed tomography: Part II. Performance study and initial results *Med. Phys.* **40** 021906

Szczykutowicz T and Mistretta C 2014 Experimental realization of fluence field modulated CT using digital beam attenuation *Phys. Med. Biol.* **59** 1305

Yartsev S, Kron T and Van Dyk J 2007 Tomotherapy as a tool in image-guided radiation therapy (IGRT): theoretical and technological aspects *Biomed. Imaging Interv. J.* **3** e16